

(NASA-TM-73805) CORRELATIONS BETWEEN  
ULTRASONIC AND FRACTURE TOUGHNESS FACTORS IN  
METALLIC MATERIALS (NASA) 18 p HC A02/MF  
A01 CSCL 11F

N78-19261

Unclas  
G3/26 09452

# **NASA TECHNICAL MEMORANDUM**

**NASA TM-73805**

**NASA TM-73805**

## **CORRELATIONS BETWEEN ULTRASONIC AND FRACTURE TOUGHNESS FACTORS IN METALLIC MATERIALS**

by Alex Vary  
Lewis Research Center  
Cleveland, Ohio 44135

REPRODUCED BY  
**NATIONAL TECHNICAL  
INFORMATION SERVICE**  
U. S. DEPARTMENT OF COMMERCE  
SPRINGFIELD, VA. 22161

**TECHNICAL PAPER** to be presented at the  
**Eleventh Symposium on Fracture Mechanics**  
Blacksburg, Virginia, June 12-14, 1978

CORRELATIONS BETWEEN ULTRASONIC AND FRACTURE  
TOUGHNESS FACTORS IN METALLIC MATERIALS

by Alex Vary  
National Aeronautics and Space Administration  
Lewis Research Center  
Cleveland, Ohio 44135

ABSTRACT

A heuristic mathematical basis is proposed for the experimental correlations found between ultrasonic propagation factors and fracture toughness factors in metallic materials. A crack extension model is proposed wherein spontaneous stress (elastic) waves produced during microcracking are instrumental in promoting the onset of unstable crack extension. Material microstructural factors involved in this process are measurable by ultrasonic probing. Experimental results indicate that ultrasonic attenuation and velocity measurements will produce significant correlations with fracture toughness properties and also yield strength.

INTRODUCTION

Strong incentives exist for developing nondestructive ultrasonic methods for evaluation of material properties such as fracture toughness (ref. 1). First, less expensive alternatives would be available to complement and corroborate mechanical destructive tests. Second, nondestructive techniques would be available for use on structural materials or actual hardware to assess or verify mechanical strength properties. Third, from the standpoint of materials science, continued ultrasonic studies should contribute to identification and analysis of factors that determine fracture toughness and thus aid in fracture control technology.

Recent studies have yielded experimental evidence that nondestructive ultrasonic methods can be used to evaluate material fracture toughness properties (ref. 2). The present study is based in part upon results reported in reference 2. The previous work demonstrated that ultrasonic attenuation and velocity measurements can be used to obtain an empirical correlation with fracture toughness properties. The purpose of the present paper is to suggest a heuristic basis for the empirical relations reported in reference 2. The material

presented should encourage further investigations and more rigorous formulations of the possible relations involved.

A model (fig. 1) is proposed for the correlations that have been found between ultrasonic propagation and fracture toughness properties of metallic materials. The model is based on stress (elastic) wave interactions during microcracking and void coalescence. (This discussion is limited to materials that fracture predominantly by void coalescence upon application of external stresses.) In the model, the formation and coalescence of microcracks are presumed to be promoted by stress wave interactions.

Equations are derived using ultrasonic quantities that are known to correlate with material fracture toughness and yield strength, that is, a material's ultrasonic attenuation coefficient and stress wave velocity. It is shown that the first derivative of the attenuation coefficient relative to frequency will correlate strongly with fracture toughness factors, for example, a material's plane strain fracture toughness value. Experimental results are cited to demonstrate the mathematical correlations with 200 and 250 grade maraging steels and a titanium alloy with the composition Ti-8Mo-8V-2Fe-3Al.

## SYMBOLS

Fundamental SI dimensions appear in parentheses.

$E$	Young's modulus, $(\text{N}/\text{m}^2)$
$\mathcal{E}$	stress wave energy, $(\text{N}/\text{m})$
$\mathcal{E}_\delta$	stress wave emission energy, $\text{J}/\text{m}^2$ , $(\text{N}/\text{m})$
$f$	frequency, $\text{MHz}$ , $(\text{s}^{-1})$
$G_c$	critical energy release rate, $(\text{N}/\text{m})$
$K_c$	critical stress intensity factor, $(\text{Nm}^{-3/2})$
$K_{Ic}$	plane strain fracture toughness, $\text{MPa}\sqrt{\text{m}}$ , $(\text{Nm}^{-3/2})$
$l$	microstructural spacing distance, $\mu\text{m}$ , $(\text{m})$
$v_l$	longitudinal velocity, $\text{cm}/\mu\text{s}$ , $(\text{m}/\text{s})$
$\alpha$	attenuation coefficient, $\text{Np}/\text{cm}$ , $(\text{m}^{-1})$
$\beta$	attenuation slope, $=d\alpha/df$ , $(\text{s}/\text{m})$
$\beta_\delta$	attenuation slope at $f = v_l/\delta$ , $\mu\text{s}/\text{cm}$ , $(\text{s}/\text{m})$

$\beta_1$	attenuation slope at $\alpha = 1$ , $\mu\text{s/cm}$ , (s/m)
$\delta$	microfracture site dimension, $\mu\text{m}$ , (m)
$\delta'$	critical grain/subgrain size, $\mu\text{m}$ , (m)
$\delta_c$	critical crack opening displacement, $\mu\text{m}$ , (m)
$\sigma_o$	initial stress wave amplitude, (N/m <sup>2</sup> )
$\sigma_w$	stress wave amplitude, (N/m <sup>2</sup> )
$\sigma_y$	yield strength, (N/m <sup>2</sup> )
$\sigma_{0.2}$	0.2 percent elongation yield strength, MPa, (N/m <sup>2</sup> )

### BACKGROUND AND APPROACH

Fracture toughness is expressed as a critical stress intensity factor  $K_c$ . It is related to the tensile modulus and critical "strain energy release rate"  $G_c$  (refs. 1 and 3),

$$K_c^2 = E' G_c \quad (1)$$

The quantity  $E'$  equals  $E$  (Young's modulus) for plane stress and  $E/(1 - \nu^2)$  for plane strain conditions, where  $\nu$  is Poisson's ratio. The quantity  $G_c$  is related to yield strength  $\sigma_y$  (ref. 3),

$$G_c = n \delta_c \sigma_y \quad (2)$$

where  $\delta_c$  is called a "critical crack opening displacement" (ref. 3) and  $n$  is a numerical coefficient. The coefficient  $n$  incorporates strain and associated factors. To determine  $K_{Ic}$  (the plane strain fracture toughness) a crack-notched specimen of suitable dimensions is loaded until the crack becomes unstable and extends abruptly.

During unstable crack growth, the stress wave propagation properties of the material are significant. Ultrasonic attenuation measurements gauge factors that influence crack propagation and hence fracture toughness. A linkage among fracture toughness, ultrasonic attenuation, and wave propagation has been shown experimentally in previous studies (refs. 2, and 4 to 6). Stress waves (i. e., acoustic emissions) in metals are emitted by dislocation motions, microcracking, etc. (refs. 4 and 5). Acoustic emission studies support the expectation that in high toughness materials the intensity of stress waves is

reduced by the ultrasonic attenuation properties of the material (ref. 6).

Ultrasonic attenuation is given in terms of the attenuation coefficient. The total attenuation coefficient is the sum of the absorption attenuation coefficient and the scattering attenuation coefficient (refs. 7 and 8). The attenuation coefficient  $\alpha$  is a function of ultrasonic frequency. Material microstructural variations will produce corresponding variations in the slope of the  $\log \alpha$  versus  $\log f$  curve (refs. 2 and 7). According to reference 2, a material's fracture toughness will vary directly with  $\beta$ , where  $\beta = d\alpha/df$ . For the analytical treatment herein, the attenuation versus frequency relation will be taken as,

$$\alpha = cf^m \quad (3)$$

This form assumes that scatter attenuation dominates and that  $m$  and  $c$  can be considered constants over the frequency range of interest.

The model (fig. 1) considers a solid under external load in which the presence of a stress raiser (i. e., imperfection, crack, notch, inclusion, etc.) gives rise to a highly stressed region. Let the load be just under that required to initiate unstable crack propagation in the neighborhood of the stress raiser or imperfection. Either of two events can arise upon slight increase of the load: First, microcrack nucleations will be initiated at various sites near the imperfection but these will fail to coalesce due to barrier effects. Second, microcrack coalescence will occur overcoming all barriers to rapid unstable crack extension.

It is assumed that the spontaneous stress (elastic) waves emitted by the various nucleation (microfracture) events interact with other potential nucleation sites and thus tend to promote fracturing at these sites. The energy of these waves will also be dissipated in the medium between nucleation sites. The propagation and energy losses of the waves would be influenced by scatter attenuation that occurs because of the presence of grain boundaries, inclusions, and other centers.

The interaction and influence of ultrasonic elastic waves on crack propagation has been well documented. By using shock stressing techniques, it has been shown that sustained crack growth occurs at times when the stress wave front is at the crack tip (ref. 9). Terminal crack speed is bounded by the stress wave's propagation velocity. Since crack speeds are less than ultrasonic wave velocities, stress wave reflections can interact with and influence the growth of a running crack (ref. 9). It has been shown that imposition of ultrasonic waves will deflect a running crack in a predictable manner (ref. 10). Other studies have

demonstrated the effect of stress wave fronts on brittle fracture (refs. 11 and 12).

### MODEL AND DERIVATION

Consider two small bounded domains (S) and (R) in a solid. These are potential crack nucleation sites near the tip of a sharp notch or crack. They share a common dimension  $\delta$  and are separated by a spacing  $\ell$  as in figure 1.

Let (S) and (R) represent two crystals, grains, or subgrains in a polycrystalline solid. They are imbedded in an assumed stress field,  $\sigma_f$ , that arises because of an externally applied load. Let (S) be the source of a stress wave that impinges on (R) as a result of a fracture in (S). The stress wave emitted by (S) is represented in figure 1 by the velocity  $v$  and stress wave amplitude  $\sigma_x$ . The arrival of the wave at (R) increases the stress field locally by  $\sigma_w$ . The magnitude of  $\sigma_w$  will be determined by attenuation which in turn will depend on the number and size of (grain) boundaries encountered by the stress wave between (S) and (R). If the wave is attenuated like any ultrasonic wave, then its amplitude at (R) where  $x = \ell$ , can be taken as,

$$\sigma_w = \eta \sigma_0 \exp(-\alpha \ell) \quad (4)$$

where,  $\eta$  is a numerical factor  $>0$  and  $<1$  that accounts for wave front geometry (and taken here as being about 1). The quantity  $\sigma_0$  is the initial stress amplitude at (S) and  $\alpha$  is the attenuation coefficient characteristic of the material.

In view of the results reported in reference 2, we first form an expression that relates the fracture toughness factor  $K_{Ic}^2/\sigma_y$  and the ultrasonic factor  $v\beta_\delta$ , where the factor  $v\beta_\delta$  is based on a particular ultrasonic frequency. It will be seen that a material's grain size is an important parameter to be used in determining this ultrasonic frequency.

Let the stress wave energy required to create a microcrack of "diameter"  $\delta$  in (R) be (ref. 13),

$$\mathcal{E} = \pi \delta \sigma_w^2 / E' \quad (5)$$

By fracturing (S) becomes the source of a broadband stress wave pulse. The wave arriving at (R),  $\sigma_w$ , will therefore contain an energy distribution corresponding to the component frequencies (ref. 4). The derivative of this energy with respect to wavelength  $\lambda$  is,

$$d\mathcal{E}/d\lambda = 2\pi\sigma_w^2 \delta \ell v \beta / E' \lambda^2 \quad (6)$$

where equation (6) is obtained by recalling that  $\beta = d\alpha/df$  and  $df/d\lambda = -v/\lambda^2$ . The component wavelengths will be scattered depending on the  $\lambda$  to  $\delta$  ratios. The energy loss by Rayleigh scattering of the stress wave on reaching (R) is,

$$\mathcal{E} = 2\pi\sigma_w^2 \delta \ell v / E' \int_{\delta}^{\infty} (\beta/\lambda^2) d\lambda \quad (7a)$$

or,

$$\mathcal{E}_{\delta} = (2\pi\sigma_w^2 \ell / E') (v\beta_{\delta}/m) \quad (7b)$$

The integration was performed by taking  $\sigma_w$  and  $v$  as material constants. The quantity  $\sigma_w$  is the critical stress increment required to initiate crack nucleation in (R) given the static field stress  $\sigma_f$ . In equation (7b)  $\beta_{\delta}$  is  $\beta$  evaluated at the frequency corresponding to  $\lambda = \delta$ . The limits of integration cover all wavelengths susceptible to Rayleigh scattering, that is,  $\lambda > \delta$ . The lower limit  $\delta$  is the criterion for stochastic scattering. It is assumed that only wavelengths less than  $\delta$  will interact strongly with the medium from (S) to (R).

At the onset of unstable crack growth, the region around (S) and (R) is loaded with a specific energy represented by  $K_c^2/\sigma_y$  (ref. 1). This energy input is accompanied by a sudden displacement in the direction of loading. This displacement can be taken as  $\delta_c$ , as measured by a COD (crack opening displacement) gauge for example (ref. 3). It is also accompanied by acoustic emissions, that is, stress wave emissions (ref. 5). The largest portion of the stress wave energy will be dissipated in the immediate vicinity of the sources such as (S) and (R) by stochastic scattering and absorption. Only the longer wavelengths  $\lambda > \delta$  appear as acoustic wave emissions beyond this region. The latter is the energy radiated away and is represented by  $\mathcal{E}_{\delta}$  in equation (7b). It is a small fraction of  $K_c^2/\sigma_y$ . Thus  $N\mathcal{E}_{\delta}$  is set equal to  $K_c^2/\sigma_y$ ,

$$(K_c^2/\sigma_y)^2 = N2\pi\sigma_w^2 n\delta_c \ell (v\beta_{\delta}/m) \quad (8)$$

where  $N \gg 1$  and equation (8) is obtained by noting that  $E'$  in equation (7b) is equal to  $K_c^2/n\delta_c\sigma_y$  by combining equations (1) and (2). The relation between the fracture toughness factor  $K_c^2/\sigma_y$  and the ultrasonic factor  $v\beta_{\delta}/m$  is, therefore,

$$K_c^2/\sigma_y = \psi(v\beta_\delta/m)^{0.5} \quad (9)$$

In practice we can take  $K_c$  as the plane strain fracture toughness  $K_{Ic}$  and  $\sigma_y$  as the 0.2 percent yield strength  $\sigma_{0.2}$ . Note that  $\sigma_{0.2}$  is related to  $K_{Ic}$  in that it corresponds to the onset of plastic deformation just as  $K_{Ic}$  corresponds to the onset of rapid fracturing. The longitudinal ultrasonic velocity  $v_\ell$  will be used for  $v$  in  $v\beta_\delta$ . The quantities  $v_\ell$ ,  $\beta_\delta$ , and  $m$  are obtained by measurements such as those described in reference 2. Equation (9) can then be written in terms of the above-mentioned quantities:

$$K_{Ic}^2/\sigma_{0.2} = \psi(v_\ell\beta_\delta/m)^{0.5} \quad (10)$$

The quantity,

$$\psi = (2\pi N n \delta_c \ell)^{0.5} \sigma_w \quad (11)$$

can be estimated by specifying particular materials and test conditions. In the next section under DISCUSSION it will be seen that the relation in equation (10) agrees with experimental observations.

## DISCUSSION

We can assign approximate "ballpark" values to the factors that constitute the quantity  $\psi$  (eq. (11)). The procedure will be to determine the bounds on  $\psi$  and to show that the available experimental data falls within these bounds. By this procedure, it will be seen that equation (10) is a valid relation between  $K_{Ic}^2/\sigma_{0.2}$  and  $v_\ell\beta_\delta/m$ .

Data for plotting  $K_{Ic}^2/\sigma_{0.2}$  versus  $v_\ell\beta_\delta/m$  are listed in table I for materials for which appropriate experimental values are available: a 200 and a 250 grade maraging steel and a titanium alloy. The quantity  $\beta_\delta$  was calculated from  $mc(v_\ell/\lambda)^{m-1}$  where  $\lambda$  is set equal to a critical grain size dimension  $\delta'$ . This critical dimension  $\delta'$  is based on measurement of grain or subgrain sizes of the various specimens by metallographic techniques. The approach adopted for determining  $\delta'$  is that of finding the dimension that best characterizes the size of potential crack nucleation sites. It is assumed that this should be the average size of the most abundant grains, their boundaries, or inclusions. For example, the titanium alloy specimens exhibited an orderly grain structure (fig. 2(a)). The typical grain size distribution for this material is shown in



figure 3. In the titanium alloy the average size varied from 59 to 64 micrometers. The 200 and 250 grade maraging steel specimens exhibited a somewhat chaotic grain-subgrain structure (fig. 2(b)). For these materials the mean subgrain boundary or lath spacing was taken as  $\delta'$  giving values ranging from 8 to 14 micrometers. The value of  $\delta'$  for each specimen is listed in table I. These measurements of  $\delta'$  were made in accordance with the intercept method prescribed in ASTM Standard E-112 (ref. 14).

It might be noted that the metallographic method for determining the critical grain size is not the only possible method for finding this important quantity. For the materials studied there is a correlation between velocity  $v_l$  and  $\delta'$ , as is shown in figure 4. The relations in figure 4 can therefore be used to ultrasonically confirm the  $\delta'$  values obtained by metallographic measurements.

The experimental data for  $K_{Ic}^2/\sigma_{0.2}$  versus  $v_l \beta_\delta/m$  are plotted in figure 5. A curve for the data as determined by linear regression is given by,

$$K_{Ic}^2/\sigma_{0.2} = 1.11 \times 10^7 (v_l \beta_\delta/m)^{0.44} \quad (12)$$

Coplotting in figure 5 are the boundary values of  $\psi$  based on the estimations given in the appendix:  $\psi = 4.5$  to  $21 \text{ MJ/m}^2$ . It is evident that  $v_l \beta_\delta/m$  and  $K_{Ic}^2/\sigma_{0.2}$  correlate well irrespective of the materials involved. A single curve, as in figure 5, seems to fit the data, at least over the range of experimental values available. The slope of this curve agrees closely with that indicated by equation (10), that is, the exponents on  $v_l \beta_\delta/m$  in equations (10) and (12) are approximately the same. The outer bounds on  $\psi$  are seen to encompass the experimental data.

The experimental results of reference 2 also suggest a linear relation of the form,

$$\sigma_{0.2} + AK_{Ic} + B\beta_1 = C \quad (13)$$

where A, B, and C are dimensional constants. Note that the terms in equation (13) will have the dimensions of specific energy (e. g.,  $\text{J/m}^2$ ) if each is multiplied by a characteristic length such as  $\delta$ . The quantities A, B, and C will assume different values according to the material involved. The ultrasonic factor  $\beta_1$  is evaluated at the frequency for which  $\alpha = 1$ . (In ref. 2 it was found that eq. (13) holds if  $\beta_1$  appears in the third term.)

The experimental relations given in reference 2 are as follows:

For the 200 grade maraging steel,

$$\sigma_{0.2} + 17K_{Ic} - 17 \times 10^3 \beta_1 = 1470 \pm 20 \quad (14a)$$

For the titanium alloy (Ti-8Mo-8V-2Fe-3Al),

$$\sigma_{0.2} - 8.1K_{Ic} + 8.1 \times 10^3 \beta_1 = 1200 \pm 13 \quad (14b)$$

The values of A, B, and C in equations (14a) and (14b) are based on data that appear in table I.

The coefficient of  $K_{Ic}$  in equation (14) or A in equation (13) will be positive or negative depending on the mode of fracture. (The algebraic sign of B will be opposite that of A.) According to data presented in reference 2, if the fracture is predominantly ductile as in the 200 grade maraging steel, then A will be positive. If brittle fracture predominates as in the titanium alloy, then A will be negative. This may depend upon the residual strain in the crack nucleation sites or whether the crack nucleation sites are energy "sources" or "sinks" during fracture.

The experimental curves of equations (14a) and (14b) are plotted as  $\sigma_{0.2}$  versus a in figure 6(a), where, the quantity  $a = \beta_1 + (A/B)K_{Ic}$ . The 0-intercept values of the two curves in figure 6(a) correspond to C. Figure 6(b) is a conventional plot of  $\sigma_{0.2}$  versus  $K_{Ic}$ .

The foregoing observations indicate that nondestructive ultrasonic measurements can be used to deduce fracture toughness and yield strength values by simultaneous solution of pairs of equations, such as equations (10) and (14a), if the ultrasonic factors  $\beta_1$  and  $v_l \beta_\delta / m$  are known. Other data would be needed to evaluate the latter factor, for example, the material and its critical micro-properties such as the value of  $\delta'$ . Ultrasonic methods such as those described in references 2 and 7 can produce this additional information. For the materials involved in this study it happened that the critical grain size as measured from photomicrographs resulted in a correlation with velocity, see figure 4. It thus appears that all the essential information for determining fracture toughness and yield strength can be obtained by purely ultrasonic measurements.

Current technical literature indicates the need for analytical treatments of fracture processes that are based on stress wave dynamics (refs. 9 to 12, 15, and 16). More emphasis should be given to the current research in crack extension dynamics under the influence of both spontaneous (internal) and externally introduced stress waves. In situ ultrasonic monitoring of unstable crack initiation (ref. 17) should play a significant role in future investigations. In the past,

a material's fracture toughness has been based on concepts that involve essentially static situations. It has now been demonstrated that considerably more insight can be gained by ultrasonic interrogation of materials, especially under dynamic conditions. As indicated by the results herein, key material properties such as fracture toughness and yield strength are closely linked to ultrasonic wave propagation properties.

## CONCLUSIONS

It has been shown that fracture toughness and yield strength are functions of ultrasonic stress wave propagation factors in polycrystalline metallic materials. It can be inferred that spontaneous stress waves generated during crack nucleation processes play an active part in promoting the onset of rapid unstable crack extension. In the model proposed herein, the formation and coalescence of microcracks are presumed to be promoted by stress wave interactions at potential crack nucleation sites. Agreement was found between the proposed model and experimental results.

Nondestructive ultrasonic measurements correlate with fracture properties and these measurements can aid significantly in identifying factors that influence catastrophic crack propagation in metallic materials. Fracture control technology should benefit by the use of nondestructive ultrasonic measurements of material microstructure properties that influence stress wave propagation and interactions.

The following conclusions can be drawn from the agreement found between the mathematical model and experimental data discussed in this paper:

1. There appears to be support for inferring that during the onset of rapid unstable crack growth, spontaneous stress waves interact with and promote crack nucleation ahead of the crack front.
2. Fracture toughness and yield strength are closely linked to the ultrasonic stress wave propagation properties of polycrystalline metals.
3. It is possible to rank material fracture toughness and yield strength by ultrasonic velocity and attenuation measurements.
4. Essential measurements for deducing fracture toughness and yield strength can be made by purely ultrasonic techniques once calibration curves have been established for a material.

APPENDIX - ESTIMATION OF " $\psi$ "

The quantity  $n$  in the expression for  $\psi$  (eq. (11)), equals 2 for plane strain conditions (ref. 3). The quantities  $N$ ,  $\delta_c$ ,  $l$ , and  $\sigma_w$  are assigned values characteristic of the materials listed in table I, that is, 200 and 250 grade maraging steel and the titanium alloy Ti-8Mo-8V-2Fe-3Al. These are the materials for which appropriate experimental data are available from reference 2.

Various measurements and estimates of acoustic emission energies (denoted as  $\mathcal{E}_\delta$ ) have been made and are of the order 800 to 900 J/m<sup>2</sup> (ref. 18). Experimental values of  $K_{Ic}^2/\sigma_{0.2}$  such as those in reference 2 indicate that the ratio of  $K_{Ic}^2/\sigma_{0.2}$  to  $\mathcal{E}_\delta$  (i. e.,  $N$ ) ranges from approximately  $1.0 \times 10^4$  to  $1.3 \times 10^4$ . The same approximate range for  $N$  can also be inferred from equation (14):  $0.81 \times 10^4$  to  $1.7 \times 10^4$ .

The critical crack opening displacement  $\delta_c$  for the materials mentioned ranges from 9 to 23 micrometers. It is calculated by solving for  $\delta_c$  between equations (1) and (2) and substituting appropriate values for  $K_{Ic}$ ,  $\sigma_{0.2}$ , and  $E$ .

The spacing dimension  $l$  is of the order of the average grain boundary spacing or greater. An estimate for  $l$  gives  $l = 30$  to 120 micrometers. This corresponds to from 2X to 3X the mean grain diameter. These values for  $l$  are determined from metallographic examination of the materials mentioned previously, see table I and the DISCUSSION section concerning the critical grain size  $\delta'$ .

The stress wave amplitude  $\sigma_w$  is taken as  $\sigma_{0.2}$ . Based on the values of  $\sigma_{0.2}$  in table I, this gives  $\sigma_w$  a range from  $1.1 \times 10^3$  to  $1.4 \times 10^3$  MPa. Using the above-assumed values for the quantities  $n$ ,  $N$ ,  $\delta_c$ ,  $l$ , and  $\sigma_w$ , the estimated outer bounds on  $\psi$  are 4.5 to 21 MJ/m<sup>2</sup>.

## REFERENCES

1. Committee on Rapid Inexpensive Tests for Determining Fracture Toughness, National Materials Advisory Board; Commission on Sociotechnical Systems, National Research Council, "Rapid Inexpensive Tests for Determining Fracture Toughness," NMAB-328, National Academy of Sciences, 1976.
2. Vary, A., "Correlations Among Ultrasonic Propagation and Fracture Toughness Properties of Metallic Materials," NASA TM X-71889, 1976.
3. Hahn, G. T., Kanninen, M. F., and Rosenfeld, A. R., in Annual Review of Materials Science, vol. 2, R. A. Huggins, Ed., Annual Reviews Inc., Palo Alto, California, 1972, pp. 381-404.
4. Liptai, R. G., Harris, D. O., Engle, R. B., and Tatro, C. A., International Journal of Nondestructive Testing, Vol. 3, Dec. 1971, pp. 215-275.
5. Tetelman, A. S. and Chow, R. in Acoustic Emission, ASTM STP-505, American Society for Testing and Materials, 1972, pp. 30-40.
6. Nakamura, Y., Veach, C. L., and McCauley, B. O. in Acoustic Emission, ASTM STP-505, American Society for Testing and Materials, 1972, pp. 164-186.
7. Papadakis, E. P., Journal of the Acoustical Society of America, Vol. 37, No. 4, Apr. 1965, pp. 711-717.
8. Krautkramer, J., and Krautkramer, H., Ultrasonic Testing of Materials, Translation of the Second Revised German Ed. by Dipl. - Ing. B. W. Zenzinger, Springer-Verlag, New York, 1969, pp. 89-121.
9. Kolsky, H., and Rader, D., in Fracture - An Advanced Treatise, Vol. 1, Microscopic and Macroscopic Fundamentals, H. Liebowitz, Ed., Academic Press, New York, 1971, pp. 533-569.
10. Kerkhof, F., in Dynamic Crack Propagation, Proceedings of an International Conference, G. C. Sih, Ed., Noordhoff International Publishing, Leyden, The Netherlands, 1973, pp. 3-29.
11. Kolsky, H., in Dynamic Crack Propagation, Proceedings of an International Conference, G. C. Sih, Ed., Noordhoff International Publishing, Leyden, The Netherlands, 1973, pp. 399-414.
12. van Elst, H. C., in Dynamic Crack Propagation, Proceedings of an International Conference, G. C. Sih, Ed., Noordhoff International Publishing, Leyden, The Netherlands, 1973, pp. 283-329.
13. Petch, N. J., "Metallographic Aspects of Fracture," in Fracture - An Advanced Treatise, Vol. 1, Microscopic and Macroscopic Fundamentals, H. Liebowitz, Ed., Academic Press, New York, 1968, pp. 351-393.

14. Standard Methods for Estimating the Average Grain Size of Metals, ASTM Standard E 112-63, in 1973 Annual Book of ASTM Standards, Part 31, American Society for Testing and Materials, 1973, p. 422.
15. Kolsky, H., Stress Waves in Solids, 2nd. ed., Dover, New York, 1963.
16. Curran, D. R., Seaman, L., and Shockey, D. A., Physics Today, Vol. 30, No. 1, Jan. 1977, pp. 46-55.
17. Klima, S. J., Fisher, D. M., and Buzzard, R. J., Journal of Testing and Evaluation, JTEVA, Vol. 4, No. 6, Nov. 1976, pp. 397-404.
18. Mirabile, M., Non-Destructive Testing, Vol. 8, No. 2, Apr. 1975, pp. 77-85.

TABLE I. - CHARACTERISTICS OF FRACTURE TOUGHNESS ULTRASONIC SPECIMENS<sup>a</sup>

Specimen	Toughness factors <sup>b</sup>			Ultrasonic (stress wave) factors <sup>c</sup>					Critical grain size, $\delta'$ , $\mu\text{m}$
	Yield strength, $\sigma_{0.2}$ MPa	Fracture toughness, $K_{Ic}$ , MPa $\sqrt{\text{m}}$	Energy factor, $K_{Ic}^2/\sigma_{0.2}$ , MJ/m <sup>2</sup>	Elastic velocity, $v_l$ , cm/ $\mu\text{s}$	Attenuation curve parameters		Attenuation factors		
					c	m	$\beta_1$ , $\mu\text{s}/\text{cm}$	$v_l \beta_\delta / \text{m}$	
e <sub>1-200</sub>	1320	(113)	9.67	0.564	$2.22 \times 10^{-3}$	2.061	0.1063	0.787	13
2-200	1430	98.1	6.73	.563	$3.46 \times 10^{-3}$	1.896	.0955	.449	13
3-200	1430	92.3	5.96	.564	$5.28 \times 10^{-3}$	1.760	.0894	.284	14
4-200	1330	103	7.98	.564	$2.02 \times 10^{-3}$	2.024	.0944	.494	15
5-200	1210	(110)	9.98	.558	$7.75 \times 10^{-4}$	2.255	.0941	.794	14
f <sub>1-250</sub>	1400	118	9.94	0.546	$3.81 \times 10^{-5}$	2.595	0.0514	0.626	8.5
2-250	↓	117	9.77	.543	$2.62 \times 10^{-5}$	2.661	.0505	.650	8.5
3-250		139	13.8	.556	$1.41 \times 10^{-5}$	2.996	.0720	1.40	13
4-250		146	15.2	.556	$1.56 \times 10^{-5}$	3.034	.0790	1.95	13
g <sub>1-Ti</sub>	1075	53.7	2.68	0.576	$4.38 \times 10^{-2}$	1.123	0.0693	0.0441	61
2-Ti	1370	51.0	1.90	.590	$3.98 \times 10^{-3}$	1.437	.0307	.0170	64
3-Ti	1230	59.9	2.92	.591	$2.27 \times 10^{-4}$	2.248	.0538	.0373	65
4-Ti	1085	70.0	4.52	.586	$5.63 \times 10^{-5}$	2.803	.0854	.117	63

<sup>a</sup>All data is taken from ref. 2 with the exception of the last two columns. The factor  $v_l \beta_\delta / \text{m}$  was calculated from the critical grain size  $\delta'$ . The quantity  $\delta'$  was determined in accordance with the discussion given in the text.

<sup>b</sup>Yield strengths are 0.2 percent elongation values. Fracture toughness values are for plane strain conditions. Conditional (less precise) values are in parentheses.

<sup>c</sup>The attenuation versus frequency characteristic curve parameters from ref. 2 are used to calculate  $\beta_1 = mc^{1/m}$  and  $\beta_\delta = mc(v_l/\delta')^{m-1}$ , see eq. (3).

<sup>d</sup>Longitudinal wave velocity was measured at a center frequency of approximately 30 MHz.

<sup>e</sup>200-grade maraging steel, cold rolled 50 percent and aged 8 hr at temperatures ranging from 700 to 811 K.

<sup>f</sup>250-grade maraging steel, annealed at 1090 K, air cooled, and aged 6 hr at temperatures ranging from 672 to 838 K.

<sup>g</sup>Titanium-8Mo-8V-2Fe-3Al, solution heat treated at 1144 K for 1 hr, water quenched, and aged 8 hr at temperatures ranging from 700 to 867 K.

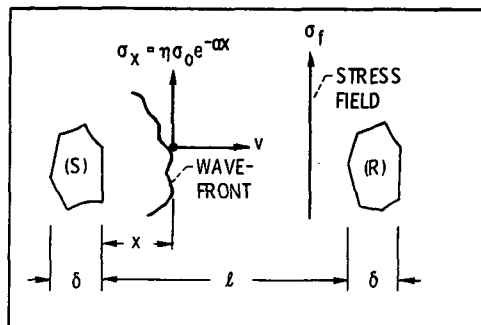
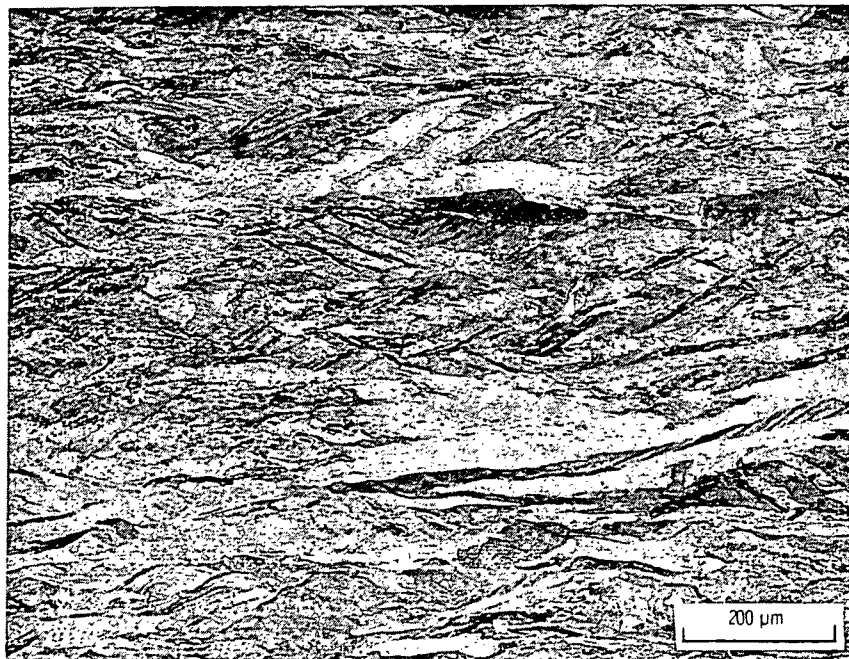


Figure 1. - Diagram of fracture model. "Grains" (S) and (R) are imbedded in a matrix subjected to a local static stress field of magnitude  $\sigma_f$ . A stress wave of initial amplitude  $\sigma_0$  and velocity  $v$  is emitted from (S). The distance between (S) and (R) is  $l$  and "grain" size is  $\delta$ .

ORIGINAL PAGE IS  
OF POOR QUALITY



(a) TANTALUM ALLOY (Ti-8Mo-8V-2Fe-3Al). ETCHANT WAS NITRIC PLUS HYDROFLUORIC.



(b) 200-GRADE MARAGING STEEL. ETCHANT WAS CALLINGS.

Figure 2. - Photomicrographs typical of two of the materials studied: a titanium alloy and a maraging steel. Original magnification was X100 for each.



ORIGINAL PAGE IS  
OF POOR QUALITY

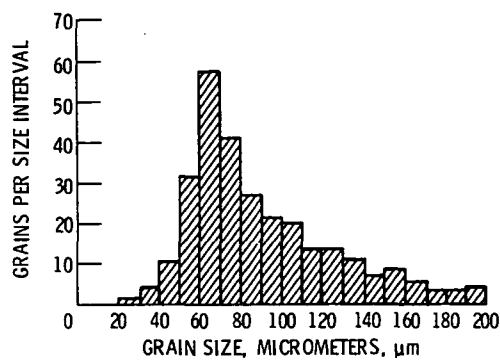


Figure 3. - Typical grain size distribution for titanium alloy Ti-2Mo-8V-2Fe-3Al. Sample population was 385.

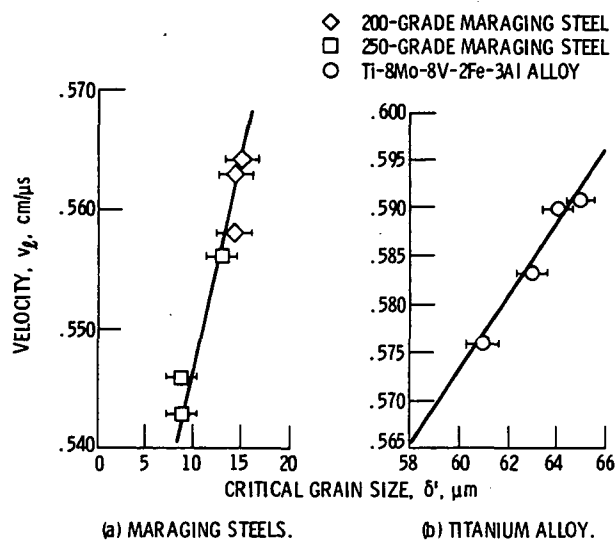


Figure 4. - Correlation of ultrasonic velocity and critical grain size for two maraging steels and a titanium alloy. Velocity measurement was at a center frequency of approximately 30 MHz.

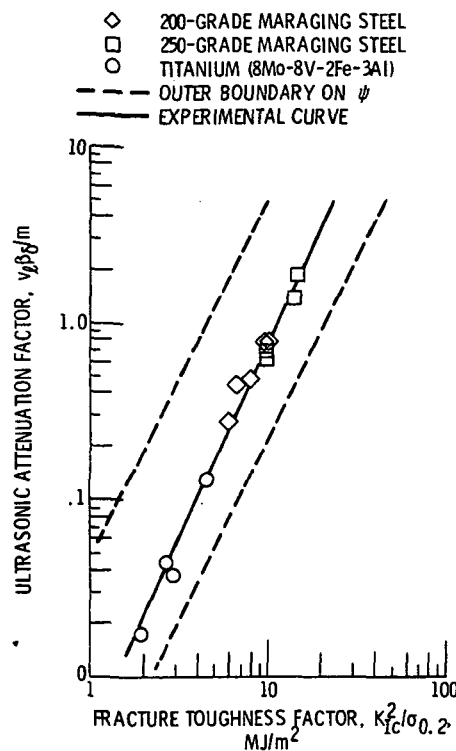


Figure 5. - Correlation of ultrasonic factor  $v_p \beta_d / m$  and fracture toughness factor  $K_{IC}^2 / \sigma_{0.2}$  for three metals. The experimental curve is based on eq. (12) and data in table I. The outer bounds on  $\psi$  are based on the estimates in the appendix and an exponent of 0.5, eq. (10).

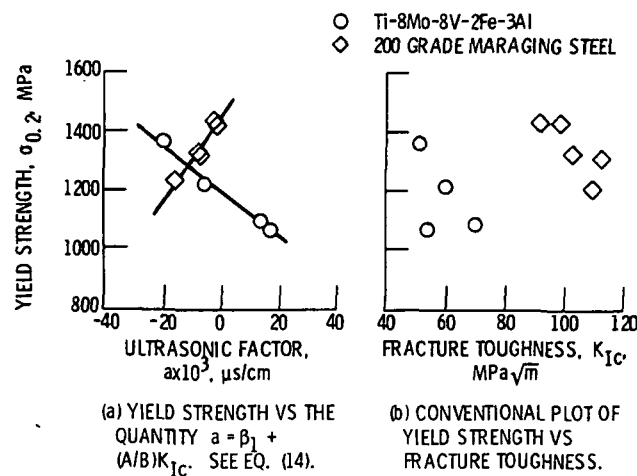


Figure 6. - Correlation of yield strength to fracture toughness for a titanium alloy and a maraging steel (from ref. 2). Refer to table I for experimental data for  $\sigma_{0.2}$ ,  $K_{IC}$ , and  $\beta_1$ .